

NON-LTE MODEL ATOM CONSTRUCTION

Norbert Przybilla¹

Abstract. Model atoms are an integral part in the solution of non-LTE problems. They comprise the atomic input data that are used to specify the statistical equilibrium equations and the opacities and emissivities of radiative transfer. A realistic implementation of the structure and the processes governing the quantum-mechanical system of an atom is decisive for the successful modelling of observed spectra. We provide guidelines and suggestions for the construction of robust and comprehensive model atoms as required in non-LTE line-formation computations for stellar atmospheres. Emphasis is given on the use of standard stars for testing model atoms under a wide range of plasma conditions.

1 Introduction

Astrophysical plasmas like stellar atmospheres, gaseous nebulae or accretion disks are not in any sense closed systems, as they emit photons into interstellar space. Therefore, the thermodynamic state of such plasmas is in general not described well by the equilibrium relations of statistical mechanics and thermodynamics for local values of temperature and density, i.e. by local thermodynamic equilibrium (LTE). The presence of an intense radiation field, which in character is very different from the equilibrium Planck distribution, results in deviations from LTE (non-LTE) because of strong interactions between photons and particles. The thermodynamic state is then determined by the principle of statistical equilibrium. All microscopic processes that produce transitions from one atomic state to another need to be considered in detail via the rate equations. A fundamental complication is that the distribution of the particles over all available energy states – the level populations or occupation numbers – in turn affect the radiation field via the effects of absorptivity and emissivity on the radiation transport. What is required is a self-consistent simultaneous solution of the radiative transfer and statistical equilibrium equations.

¹ Dr. Remeis-Sternwarte Bamberg & ECAP, Astronomisches Institut der Universität Erlangen-Nürnberg, Sternwartstrasse 7, D-96049 Bamberg, Germany

A *model atom* is a collection of atomic input data required for the numerical solution of a given non-LTE problem. It is a *mathematical-physical approximation* to the quantum-mechanical system of a real atom, and its interaction with radiation and with other particles in a plasma. A model atom comprises, on one hand, data to specify the structure of the atom/ion like energy levels, statistical weights and ionization potentials. On the other hand, the transitions among the individual states need to be described, requiring oscillator strengths, cross-sections for photoionization and collisional excitation/ionization, etc. The number of levels in a model atom amounts typically to several tens to several hundred in modern work, and the number of transitions from hundreds to many (ten-)thousands.

As only a very limited amount of atomic data have been determined experimentally up to now – mostly energy levels, wavelengths and oscillator strengths –, most of the data have to be provided by theory. Large collaborative efforts have been made to compute the data required in astrophysical applications via *ab-initio* methods. The Opacity Project (OP; Seaton 1987; Seaton et al. 1994) and its successor the IRON Project (IP; Hummer et al. 1993) provided enormous databases of transition probabilities and cross-sections for photoionization and excitation via electron impact. Many smaller groups and individuals have contributed additional data, most notably Kurucz (see e.g. Kurucz 2006) in a tremendous effort lasting already for about three decades. *Ab-initio* data for radiative processes between levels of principal quantum number $n \leq 10$ are available for most of the ions of the lighter elements up to calcium, and for iron. *Ab-initio* data for excitation via electron collisions are by far less complete, typically covering transitions up to $n \leq 3$ or 4 for selected ions of the lighter elements and for iron. Reliable data for other members of the iron group and for the heavier elements are only selectively available. The remainder of data – still the bulk by number – has to be approximated for practical applications.

Consequently, the starting point for the construction of model atoms for many elements of astrophysical interest has improved tremendously since the mid-1980s. Nevertheless, building realistic model atoms is neither an easy nor a straightforward task. It is a common misconception that non-LTE *per se* brings improvements over LTE modelling. A careful LTE analysis of well-selected lines *can* be more reliable than a non-LTE study of the ‘wrong’ lines with an inadequate model atom. On the other hand, computations using a realistic model atom *will* improve over LTE – provided that the other ingredients of the modelling are also realistic.

The independence of microscopic processes from environment – at least under not too extreme conditions – provides a tool to assess the quality of model atoms by comparison with observation. Comprehensiveness and robustness of a model atom are given when it reproduces the observed line spectra over a wide range of plasma conditions. Standard stars should serve as test ‘laboratories’, covering a wide range of effective temperature and surface gravity (particle density).

In the following we discuss practical aspects of the construction of model atoms for non-LTE line-formation calculations of trace elements in stellar atmospheres. Guidelines and suggestions are given how to build up robust and comprehensive model atoms, and how to test them thoroughly.

2 Problem Definition

Non-LTE line-formation calculations solve the coupled statistical equilibrium and radiative transfer equations for a prescribed model atmosphere, which may itself be in LTE or non-LTE. The computational expenses are therefore lower than for full non-LTE calculations that solve also for the atmospheric structure. Hence, comprehensive model atoms may be treated in great detail, which turns out to be a crucial advantage of restricted non-LTE calculations.

One of the most important quantities for the comparison with observed spectral lines – which is the basis of quantitative spectroscopy – are *accurate occupation numbers* n_i for the levels involved in the transitions. These have to be determined in general by solution of the rate equations of statistical equilibrium (though detailed equilibrium may turn out a valid approximation *a posteriori*)

$$\sum_{j \neq i} n_i (R_{ij} + C_{ij}) = \sum_{j \neq i} n_j (R_{ji} + C_{ji}), \quad (2.1)$$

where the R_{ij} and C_{ij} are the radiative and collisional rates, respectively, for the transitions from level i to level j . Radiative upward rates are given by

$$R_{ij} = 4\pi \int \sigma_{ij}(\nu) \frac{J_\nu}{h\nu} d\nu, \quad (2.2)$$

where $\sigma_{ij}(\nu)$ is an atomic cross-section for bound-bound or bound-free processes, J_ν the mean intensity, h Planck's constant and ν the frequency. In the case of collisional processes the upward-rates are given by

$$C_{ij} = n_e \int \sigma_{ij}(v) f(v) v dv, \quad (2.3)$$

where n_e is the electron density (for the moment we assume that collisions with heavy particles can be neglected, see Sect. 5), v the velocity and $f(v)$ the (in general Maxwellian) velocity distribution of the colliding particles. The corresponding downward rates are derived from detailed-balancing arguments, requiring correction for stimulated emission in the case of the radiative downward rates.

Inspection of Eqns. 2.1–2.3 shows which input quantities need to be reliably known in order to facilitate an accurate determination of the level populations: I) the local temperatures and particle densities, *and* II) the non-local radiation field, *and* III) accurate cross-sections σ_{ij} , *and* IV) all transitions relevant for the problem have to be taken into account. Any shortcomings in these will affect the final accuracy that can be obtained in the modelling.

Items I) and II) depend on the prescribed model atmosphere used for the restricted non-LTE calculations. This has to give a fair description of the *real* temperature gradient and the density stratification in the star's atmosphere under investigation. Particular care has to be invested in the stellar parameter determination (effective temperature T_{eff} , surface gravity $\log g$). This has to account for a self-consistent treatment of quantities which are often thought to be of secondary nature (microturbulence ξ , metallicity, helium abundance, etc.), see Nieva

& Przybilla (this volume). Good knowledge of the model atmosphere code is a prerequisite for successful non-LTE line-formation computations for individual cases – use of published model grids allows only to scratch the surface of the problem.

Items III) and IV) are related to the model atom. Nowadays, the question is often not *whether* to use *ab-initio* data for the model atom construction, but *which* of the available datasets to adopt. This is a matter of experience and familiarity with atomic physics. The quality of agreement of *ab-initio* results with available experimental data should certainly guide the decision. A first important step is to check how well the *ab-initio* calculations reproduce the observed energies of the levels in an atom/ion. A comparison of observed and computed oscillator strengths and cross-sections for reactions gives further indications (see for example reviews by Williams 1999; Kjeldsen 2006). The latter will typically be possible only for ground and metastable states, but the opportunity for constraining the accuracy of the theoretical data should not be missed. Another criterion is the agreement between length and velocity forms of oscillator strengths to verify the internal consistency of the *ab-initio* calculations. Eventually, different model atoms may be constructed using the alternatives as input data to decide empirically which dataset should be preferred for the practical work.

Experience is also the key in deciding how extended a model atom should be and which transitions should be considered. Nature realises all possibilities, but we have to handle the mathematical solution of a set of equations describing the physics packed into a (restricted) model. In particular, the numerical solution of the set of linear equations (2.1) requires to be handled carefully. Precautions need to be taken to keep the numerical problem well-conditioned and the algorithms stable. In practice this means that some transitions may better be ignored in a model atom, or the number of levels may be restricted in order to obtain meaningful results. Larger model atoms accounting for more transitions are therefore not necessarily ‘better’, even if the individual atomic input data are of high quality.

Finally, execution times of the model computations are also important for the practical work. They should not be excessive, requiring a certain compactness of model atoms even for non-LTE line-formation computations on prescribed model atmospheres. Hence, the construction of model atoms is effectively a highly complex optimisation problem. A compromise needs to be found between comprehensiveness, accuracy, stability and efficiency.

3 Model Atom Structure

The first step in the construction of a model atom is to decide on the extension of the model: which ions, which energy levels should be included, and how? This depends on the specific non-LTE problem and may range from a few levels for studies of a resonance line to many hundred – including packed ‘superlevels’ – if a reproduction of the complex spectra of e.g. iron group species is aspired. In the following we concentrate on the general strategy for the construction of comprehensive model atoms, which are able to reproduce practically the entire observed spectra of an ion over a wide parameter range.

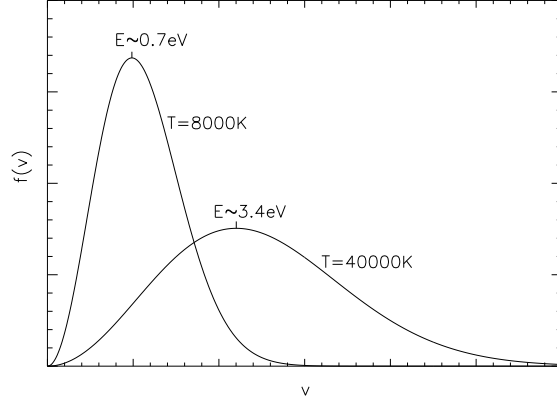


Fig. 1. Schematic plot of the Maxwellian velocity distribution for typical temperatures at line-formation depths in A- and O-type stars.

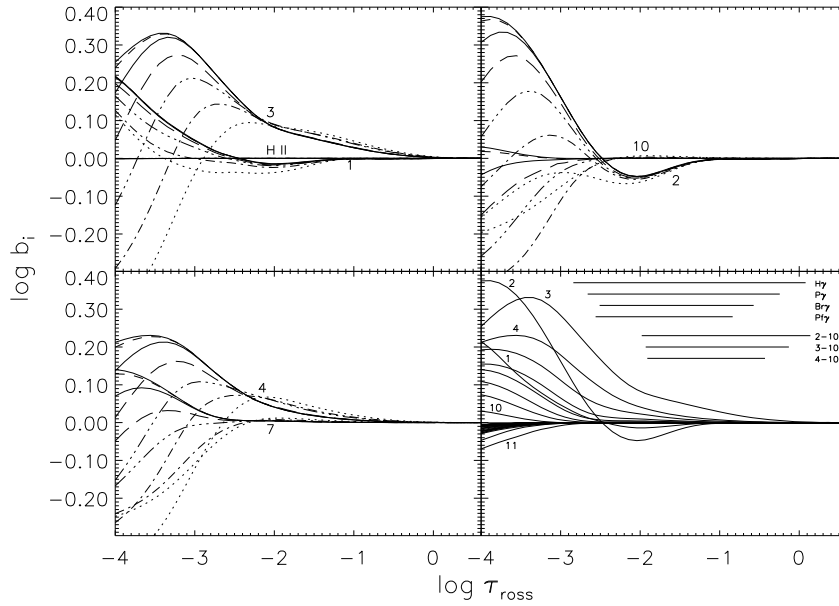


Fig. 2. Run of departure coefficients b_i in a model of the bright supergiant β Ori (B8 Ia) as a function of τ_{ross} for H I model atoms of different complexity: for 10, 15, 20, 25, 30, 40, 50 levels (dotted, dashed-dotted, dash-dot-dot-dotted, long dashed, full, dashed, full thick lines). The lower right panel displays the behaviour of all levels in the 50-level model atom. Note the Rydberg states asymptotically approaching the H II limit. See the text for details. From Przybilla & Butler (2004).

The fundamental parameter that determines which ions should be included in a model atom is the effective temperature, as this determines the energetics of the microscopic processes. The term structure of the ions provides a second criterion. Hence, the main ionization stage should be adequately represented, plus usually two or three minor ionic species – which may comprise in fact the ones of particular interest. E.g., the main ionization stage of carbon in a B0 V star (with $T_{\text{eff}} \approx 32\,000\text{K}$) is C III in the line-formation region, but features of the minor species C II and C IV are also present in the optical spectra. Consequently, a comprehensive model atom should consider C II-IV, plus the ground level of C V. The latter has an enormous energy gap between the ground and the first excited level, of about 300 eV, such that from atomic structure considerations excited C V levels can be safely ignored in the model atom. A lithium model atom for use with solar-type stars can be kept simple – detailed Li I + the Li II ground level – for the same reason, despite Li II dominating by far in terms of population.

Concerning the choice of levels to include in a comprehensive model atom there are two objective criteria available, which are tightly coupled. One is the energy gap between the energetically highest level of the ion and the continuum, as defined by the ground level of the next higher ionization stage. As a general rule the gap should be less than kT to ensure an accurate determination of ionization fractions¹. In order to keep a model atom robust it is recommended to include energetically higher levels than the minimum necessary to cope with a given problem. Non-LTE studies of the Mg II $\lambda 4481\text{ \AA}$ line may serve as an example: the line is observable from F-type to mid O-type stars. For explaining the behaviour of the line in early-type stars (Mihalas 1972) it may be sufficient to consider levels up to $n = 5$ or 6 using the criterion above, as the majority of the colliding particles will be able to facilitate ionization (see Fig. 1). However, the same model atom will not be useful for analyses of A-type stars, as only a small fraction of electrons in the high-velocity tail of the Maxwell distribution will be able to overcome the reaction threshold. In that case, completeness up to $n = 8$ would be required, etc.

The second criterion is the convergence of the behaviour of level departure coefficients b_i with increasing model complexity (for a given set of transition data). An example is shown in Fig. 2, for hydrogen model atoms considering levels up to $n = 10$ to 50. Models with a too low a number of levels can show a different behaviour at line-formation depths than the more complex models, resulting in inaccurate predictions. An alternative formulation of this criterion is via the convergence of the line source function (e.g. Sigut 1996).

For many elements fine-structure states of a term may safely be combined into one level representing the term. This comprises, in particular, the cases that are approximated well by LS -coupling. Collisions couple the individual sub-levels tightly because of their small energy separations, i.e. they are in LTE relative to each other. A similar opportunity for simplification of the model atom opens up for levels at higher excitation energies. The energy separations of terms decrease

¹Minority species are particularly sensitive to non-LTE effects because any small change of the ionization rates can affect their populations by a significant amount.

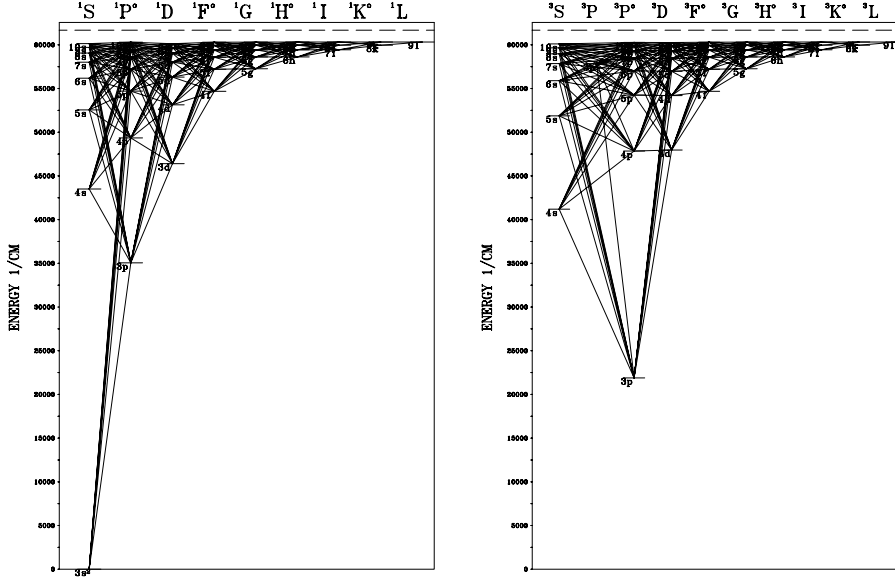


Fig. 3. Example of a comprehensive model atom structure. Grotrian diagrams for the singlet and triplet spin systems of Mg I are shown. Displayed are the radiative bound-bound transitions treated explicitly in the non-LTE calculations. The ionization threshold is indicated by the dashed line. From Przybilla et al. (2001).

with increasing angular quantum number ℓ for the same n , and in general with increasing n . Eventually, they may be safely grouped into one level with appropriate statistical weight. This helps to keep the number of explicit non-LTE levels to be treated for elements up to about calcium below ~ 200 , even if several ionization stages are treated simultaneously. An example of a comprehensive model atom structure is visualised in Fig. 3 in form of a Grotrian diagram, for Mg I. For the heavier elements with complex electron structure like the iron group elements it may be worthwhile to consider regrouping a multitude of levels with similar properties into ‘superlevels’ (and the transitions into ‘superlines’), a concept first introduced by Anderson (1989).

4 Radiative Transitions

The *non-local* character of the radiation field drives the stellar atmospheric plasma *out of detailed equilibrium*: photons can travel large distances before interacting with the particles, coupling the thermodynamic state of the plasma at different depths in the atmosphere. This affects the excitation and ionization of the material. Radiative transitions obey *selection rules*.

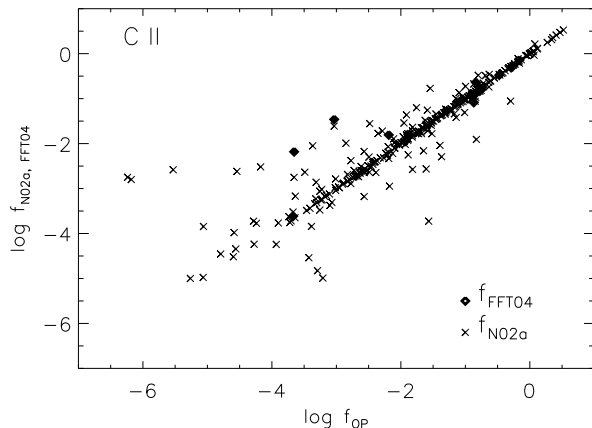


Fig. 4. Comparison of oscillator strengths for C II: values from Froese Fischer & Tachiev (2004) and Nahar (2002) vs. data from the Opacity Project (Yan et al. 1987). From Nieva & Przybilla (2008, NP08).

4.1 Line Transitions

Changes in the internal energetic state of an atom/ion can occur by the absorption/emission of photons, giving rise to spectral lines. The strength of a spectral line is basically determined by the number of absorbers (or emitters) and the line absorption cross-section, which is given by

$$\sigma_{ij} = \frac{\pi e^2}{m_e c} f_{ij} \phi(\nu), \quad (4.1)$$

where e is the electron charge, m_e the electron mass and f_{ij} the oscillator strength. $\phi(\nu)$ is the line absorption profile (the emission line profile is identical assuming complete redistribution), which can be approximated well by a Doppler profile in most cases when the coupled radiative transfer and statistical equations are solved to determine the level populations² in the restricted non-LTE approach.

The accuracy of the oscillation strengths used for the model atom construction will be a limiting factor for analyses. Fortunately, high-accuracy data is available in many cases³, obtained both from experiments as well as from *ab-initio* calculations.

It is worthwhile to cross-check available data sources. Newer data are not necessarily better, even if a apparently more advanced method was used for their determination. As usual, the devil is in the details. An example is shown in Fig. 4. Oscillator strengths for C II from the OP (*R*-matrix method in the close-coupling

²Detailed line broadening theories become important for the last step of non-LTE line-formation computations, when synthetic spectra are calculated.

³Oscillator strengths are the only ones among the atomic data discussed further on in Sects. 4–6 that are required in LTE investigations.

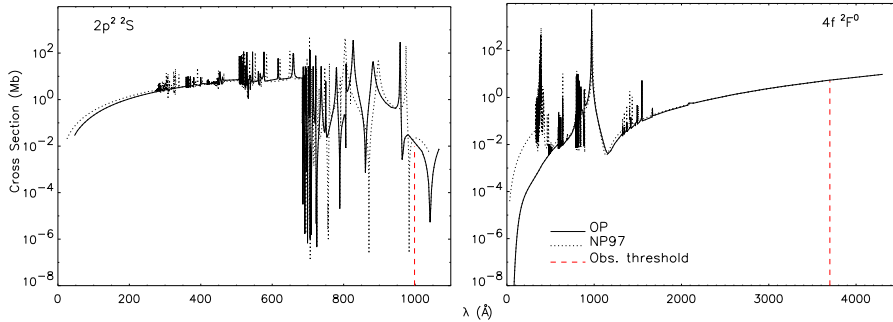


Fig. 5. Comparison of C II photoionization cross-sections from the Opacity Project (Yan & Seaton 1987) and Nahar & Pradhan (1997) for $2p^2\ ^2S$ and $4f^2\ ^2F^o$ as a function of wavelength. From NP08.

approximation assuming *LS*-coupling) are compared to data of Nahar (2002) obtained with the (in principle superior) Breit-Pauli *R*-matrix (BPRM) method and the smaller number of high-precision data from application of the Multiconfiguration Hartree-Fock (MCHF) method. The in general good agreement between the OP and the MCHF data (with few exceptions they follow the 1:1 relation) and the considerable scatter in the comparison of OP and Nahar’s *f*-values was one of the factors to disregard this particular set of BPRM data from the model atom construction in that case. However, the question which of the available data should be used for the construction of model atoms has no simple answer in general.

Limitations on the number of transitions that can be considered explicitly in the radiative transfer calculations may be imposed by the numerical method chosen for solving the equation systems. Complete linearisation techniques are much more restricted than Accelerated Lambda Iteration (ALI) techniques. The most important transitions (high *f*-value, location at wavelengths with non-negligible flux) will need to be considered in the former case while virtually all line transitions may be accounted for in the latter case, see Fig. 3 for an example.

4.2 Photoionizations

The availability of photoionization cross-sections has improved enormously in the past 20 years, mostly because of the efforts made in the OP and IP. Like for oscillator strengths, the quality of the different data sets should be evaluated for the model atom construction. A comparison of photoionization cross-sections from two different calculations is shown in Fig. 5, for two excited levels in C II. Maybe surprisingly, some details can be relevant for the model atom construction, while obvious discrepancies may be not. The small shifts in the resonance structure near the ionization threshold of the energetically relatively low-lying $2p^2\ ^2S$ state of C II (see Fig. 8 for a Grotrian diagram) can be important for the rate determination, as they occur near the flux maximum of OB-type stars. The more than two orders-of-magnitude differences in the high-energy tail of the cross-section for

the $4f^2F^\circ$ level (occurring because of the different targets in the two *ab-initio* calculations) are irrelevant on the other hand, because of the low flux at these short wavelengths. It has to be decided by comparison of the results from different model atom realisations which of the available data should finally be selected, see Sect. 7 for an example. As always, some guidance may also be obtained by comparison of the different theories with experiments.

The OP and IP have provided *ab-initio* data for photoionization from levels with typically $n \leq 10$ and $\ell \simeq 4$. Missing data for levels of higher n or ℓ may be rather safely approximated by hydrogenic cross-sections (Mihalas 1978, p.99)

$$\sigma(\nu) = 2.815 \times 10^{29} \frac{Z^2 g_{\text{II}}(n, \nu)}{n^5 \nu^3}, \quad (4.2)$$

for the model atom construction, in particular as these levels are usually packed, see Sect. 3. Here, Z denotes the charge of the ion and g_{II} the bound-free Gaunt factor, which is of order unity at ionization threshold. The threshold cross-section is given by $\sigma(\nu_0, n) = 7.91 \times 10^{-18} / Z^2 n g_{\text{II}} \text{ cm}^2$.

5 Collisional Transitions

Inelastic collisions with particles can also lead to excitation and ionization of atoms/ions. The velocity distribution of particles in stellar atmospheres is in practically all cases Maxwellian, determined by the *local* plasma temperature. Collision processes will therefore drive the plasma *towards LTE*. Contrary to radiative transitions, no selection rules apply. Typically, only electron collisions are considered, as the thermal velocity and hence the collision frequency of heavy particles is much smaller, e.g. by a factor ~ 43 for hydrogen. This is in particular valid for all environments where the stellar plasma is sufficiently ionized. Heavy particle collisions may become important in special cases, however, like for cool metal-poor stars.

5.1 Collisional Excitation

The main aspect of collisional excitation by electron impact is certainly the thermalising effect on level populations in general, dampening out departures from detailed equilibrium imposed by the radiative processes. Curiously enough, collisional excitation can also drive individual level occupations *out of LTE* under special circumstances. This occurs for cases where a level is collisionally tightly-coupled to another level that experiences strong non-LTE departures. Examples are energetically close levels from different spin systems, one being metastable (a radiative decay to the ground state is prohibited by selection rules). A prominent example for this coupling are the $3s^3S$ and $3s^5S$ levels of O I (Przybilla et al. 2000; Fabbian et al. 2009).

Larger sets of collisional excitation data for transitions up to typically $n = 3$ or 4 are available now, e.g. from the IP. A good part of the data are published in the astrophysics literature, but the reader should be aware that much more data can be found in the physics literature because of their relevance for fusion research

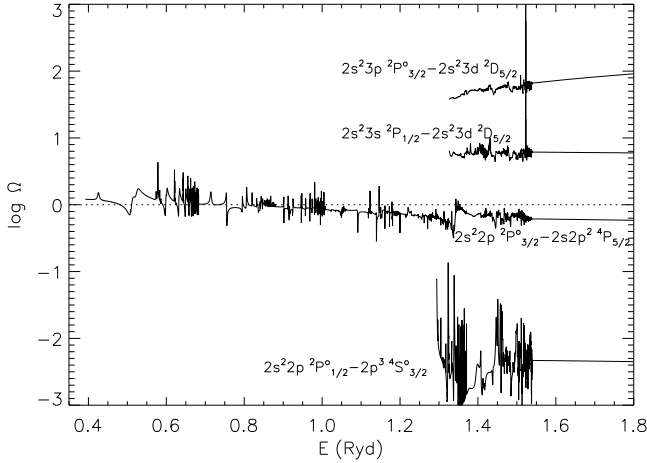


Fig. 6. Examples of collision strengths Ω for optically allowed and forbidden transitions in C II in the near-threshold region as a function of incident electron energy (fine-structure data from Wilson et al. 2005). For comparison, $\Omega = 1$ is indicated by a dotted line.

and technical applications. Most useful for practical applications are tabulations of thermally-averaged effective collision strengths

$$\Upsilon_{ij} = \int_0^{\infty} \Omega_{ij} \exp(-E_j/kT) d(E_j/kT), \quad (5.1)$$

where E_j is the energy of the outgoing electron and Ω_{ij} the collision strength, which is symmetric as well as dimensionless, $\Omega_{ij} = \Omega_{ji}$. Effective collision strengths facilitate an easy evaluation of transition rates, which are proportional to Υ_{ij} .

While *ab-initio* data are of highest relevance for the construction of model atoms, one has to resort to approximation formulae for the vast majority of possible transitions. Different descriptions are available from the literature, a comparison can be found in Mashonkina (1996). In the following we concentrate on the two most commonly used approximations.

The semiempirical formula of Van Regemorter (1962) allows rates for radiatively permitted transitions to be evaluated in terms of the oscillator strength,

$$C_{ij} = 5.465 \times 10^{-11} n_e T^{1/2} [14.5 f_{ij} (u_H^2/u_0)] \exp(-u_0) \Gamma(u_0), \quad (5.2)$$

where u_H is the ionization potential of hydrogen scaled by kT , $u_0 = E_0/kT$ (E_0 is the threshold energy for the process), and $\Gamma(u_0) \equiv \max[\bar{g}, 0.276 \exp(u_0) E_1(u_0)]$ for ions (E_1 is the first exponential integral). The parameter \bar{g} is about 0.2 if the principal quantum number changes during the transition and about 0.7 if not. For neutral atoms $\Gamma(u_0)$ has a different form (see Auer & Mihalas 1973).

Excitation rates of radiatively forbidden transitions are often evaluated according to the formula of Allen (1973),

$$\Gamma_{ij}(T) = \frac{\Omega_{ij}}{g_i} \frac{h\nu_H}{kT}, \quad (5.3)$$

where $\Gamma_{ij}(T)$ is a temperature-dependent factor in the collision rate as defined by Mihalas (1978, p. 133). Typically, $\Omega = 1$ is assumed for forbidden transitions.

Note that Eqns. 5.2 and 5.3 give, at best, order-of-magnitude estimates. Comparisons of *ab-initio* data with the approximations should be made whenever possible to evaluate the true uncertainties that can be expected. An example is shown in Fig. 6. Differences of up to several orders of magnitude are found, and the quantum-mechanical data can show pronounced resonance structure. It is therefore advisable to investigate the available *ab-initio* data for trends and regularities. Extrapolations can be made based on these in order to improve the approximate input data for the model atom construction.

5.2 Collisional Ionization

The rates of collisional ionization by electron impact are mostly affected by the availability of electrons with energies high enough to overcome the threshold for the reaction. This makes collisional ionization from the ground state and energetically low-lying levels rather inefficient, as only few electrons in the high-velocity tail of the Maxwell distribution are available for this. On the other hand, collisions become a dominant factor for the coupling of high-lying levels to the continuum.

Unfortunately, cross-sections for ionization by electron impact are among the least-constrained atomic data. Experiments usually cover ionization from the ground state only, and the reader is referred to the atomic physics literature for extracting data for a specific problem. On the theoretical side, few methods have been successfully applied. The fundamental challenge which distinguishes collisional ionization from excitation is the fact that the Coulomb interaction between each of the two outgoing electrons and the residual ion is present even at large distances. Recently, breakthrough results have been obtained by use of the converging close-coupling method. Several fundamental processes have been modelled accurately, providing cross sections that closely reproduce the available experimental data in these cases, see Bray et al. (2002) for a review.

However, in the majority of cases one has to rely on more simple approaches. An often used approximation formula for quantifying collisional ionization was given by Seaton (1962), which expresses the collisional cross-section in terms of the photoionization cross-section, yielding a rate

$$C_{i\kappa} = 1.55 \times 10^{13} n_e T^{-1/2} \bar{g}_i \sigma(\nu_0) \exp(-u_0)/u_0, \quad (5.4)$$

where $\sigma(\nu_0)$ is the threshold photoionization cross-section (Sect. 4.2), and \bar{g}_i is of the order 0.1, 0.2, and 0.3 for $Z = 1, 2$, and ≥ 3 , respectively. Again, Eqn. 5.4 provides, at best, an order-of-magnitude estimate. A comparison of collision rates

calculated with Eqn. 5.4 with those evaluated by an empirical analytical expression (Drawin 1961) indicates that the uncertainties may be sometimes much larger (Mashonkina 1996). The Seaton formula (and analogous simple approximations) should therefore be applied with caution.

5.3 Hydrogen Collisions

Excitation and ionization by inelastic heavy particle collisions are usually considered unimportant in comparison to electron collisions, which occur more frequently. However, the ratio of hydrogen atoms to electrons may easily exceed a factor 10^4 in cool stars, in particular in metal-poor objects. In such a case H collisions may become a dominant thermalisation process, which must not be neglected.

Characteristic collision energies in cool star photospheres are of the order $kT \approx 0.2 - 0.6$ eV, i.e. they are comparable to typical atomic transition energies. Consequently, the near-threshold behaviour of the cross-sections is most important for the determination of the collision rates. Laboratory measurements or *ab-initio* calculations of cross-sections near threshold are scarcely found in literature for these neutral particle collisions. Some progress has been made recently for the Na + H system (Fleck et al. 1991; Belyaev et al. 1999, 2010), showing that the collision rates can differ by several orders of magnitude compared to simple approximations (see the discussion below). Similar discrepancies were also found for the Li + H system (Belyaev & Barklem 2003).

In face of the absence of reliable data for practically all cases of interest, one has to resort to the use of approximations for the description of inelastic hydrogen collisions. Most work relies on the Steenbock & Holweger (1984) approximation, who generalised Drawin's formulae (Drawin 1968, 1969; based on Thomson's classical theory), originally developed for collisions between identical particles. The Maxwell-averaged formulae for excitation and ionization of particle species A by collision with H becomes

$$\langle \sigma v \rangle = 16\pi a_0^2 \left(\frac{2kT}{\pi\mu} \right)^{1/2} Q \frac{m_A}{m_H} \frac{m_e}{m_H + m_e} \Psi(W), \quad (5.5)$$

with $\mu = m_A m_H / (m_A + m_H)$ denoting the reduced mass. For collisional excitation $Q = (I_H / \Delta E)^2 f_{lu}$ and $W = \Delta E / kT$ and for collisional ionization $Q = (I_H / I_A)^2 f_i \xi_i$ and $W = I_A / kT$, where ΔE denotes the energy difference between upper and lower state of the transition and I_H and I_A are the ionization energy of hydrogen and atomic species A ; f_{lu} is the oscillator strength, f_i is an efficient oscillator strength for ionization and ξ_i the number of equivalent electrons. The function $\Psi(W)$ is given by $\Psi(W) = (1 + \frac{2}{W}) \exp(-W) (1 + \frac{2m_e}{(m_H + m_e)W})^{-1}$. Note that Eqn. 5.5 does not apply to optically forbidden transitions. Takeda (1991) suggested to relate the hydrogen collision rate with the electron collision rate via

$$C_{ij}^H = C_{ij}^e \frac{n_H}{n_e} \left(\frac{m_e}{\mu} \right)^{1/2}, \quad (5.6)$$

assuming *ad-hoc* a similarity of cross-sections for both cases (C_{ij}^e is usually evaluated with $\Omega = 1$). Here, n_{H} denotes the number density of neutral hydrogen.

Often the results are scaled by a factor S_{H} . A value of $S_{\text{H}} = 0$ is equivalent to no hydrogen collisions, $S_{\text{H}} \rightarrow \infty$ enforces LTE. In general, S_{H} is constrained empirically by demanding that the scatter in abundance as determined from the entire sample of lines of a species should be minimised.

Equations 5.5 and 5.6 were considered appropriate to provide an order-of-magnitude estimate for a long time, but in view of the few *ab-initio* calculations available now, this assessment appears too optimistic. This confirms earlier indications of an underestimation of the real uncertainties, from the comparison with other approximations, see e.g. Mashonkina (1996). Barklem (2007) investigated the uncertainties for the most simple case, $\text{H} + \text{H}$, in detail.

The Steenbock & Holweger formula remains in use for astrophysical applications in view of the lack of other reliable data, despite all the warning evidence. In view of this, efforts should be made to determine proper scaling factors S_{H} in order to minimise the impact on the accuracy of analyses. This could be made by extensive investigations following the recommendations for testing model atoms in Sect. 7, covering the parameter space comprehensively (wide range of effective temperature, densities and metallicity).

6 Other Processes

Consideration of the processes described in the previous two sections is usually sufficient for the construction of model atoms for the analysis of stellar photospheres. Nonetheless, two other types of radiative and collisional processes may be of relevance in some cases. They are only briefly described in the following for completeness, leaving it to the reader to investigate the specialist literature.

Autoionization can occur in complex atoms with several electrons. When two electrons are excited simultaneously, this can give rise to states below and above the ionization potential. The states above the ionization threshold may autoionize to the ground state of the ion, releasing one electron. The inverse process is also possible, and, if a stabilising radiative decay occurs within the (short) lifetime of the doubly excited state⁴, it can give rise to an efficient recombination mechanism. This is referred to as *dielectronic recombination*. Details of rate coefficient modelling can be found e.g. in Badnell et al. (2003). An application in the context of WR-type central stars of planetary nebulae is discussed by de Marco et al. (1998).

Charge exchange reactions are collisional processes between atoms/ions in which one, or more, electrons are transferred from one collision partner to the other, e.g. $\text{A} + \text{B}^+ \rightarrow \text{A}^+ + \text{B}$, with B usually being H or He. One well-known reaction occurring in stellar atmospheres is $\text{O} + \text{H}^+ \rightleftharpoons \text{O}^+ + \text{H}$, which can dominate the ionization balance of oxygen as the non-LTE departures of the $n(\text{H I})/n(\text{H II})$ are

⁴The presence of these so-called autoionizing states has consequences for the absorption of photons and the scattering of electrons by atoms/ions: it gives rise to resonances in the photoionization and electron collision cross-sections, see Figs. 5 and 6.

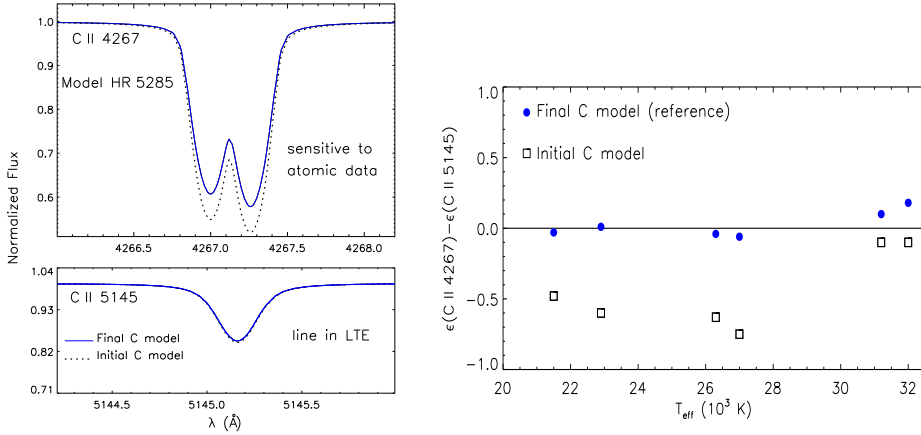


Fig. 7. Left: sensitivity of two C II lines to use of photoionization cross-sections from different *ab-initio* calculations in a model spectrum for a B2 V star. Right: differences in (logarithmic) carbon abundance as derived from the two lines in 6 stars as a function of effective temperature. From NP08.

forced upon $n(\text{OI})/n(\text{O II})$ by this resonant reaction (the ionization potentials of neutral hydrogen and oxygen are very similar), see e.g. Baschek et al. (1977) or Przybilla et al. (2000) for a discussion. A list of reaction playing a possible role in astrophysical plasmas and tabulated reaction rates are provided e.g. by Arnaud & Rothenflug (1985).

7 Testing Model Atoms

The question whether a model atom is realistic can only be answered by comparison with observation. One needs to test whether the model atom is comprehensive enough, i.e. whether the level structure and all relevant connecting transitions are considered properly and whether the atomic data used are sufficiently accurate. Usually, this should give rise to an iterative process: a stepwise improvement of the model atom by empirical selection of the ‘best’ input data. The aim is to single out *one* model atom, that reproduces the observed spectra closely *at once*, independent of the plasma conditions (atomic properties are independent of environment).

In order to give an idea on the practical approach for performing such tests we discuss an example. Synthetic line profiles from calculations with two different model atoms are compared in the left panel of Fig. 7. While the strong C II $\lambda 4267 \text{ \AA}$ transition is highly sensitive to non-LTE effects – in particular to the photoionization cross-sections adopted –, the other line is virtually insensitive to any model atom realisation using reasonable atomic input data (it is ‘in LTE’). Such a sensitivity is one of the keys to select the ‘right’ photoionization data for the model atom construction. The second ingredient in this process is the comparison with observations, here for stars in a temperature sequence (right panel of Fig. 7).

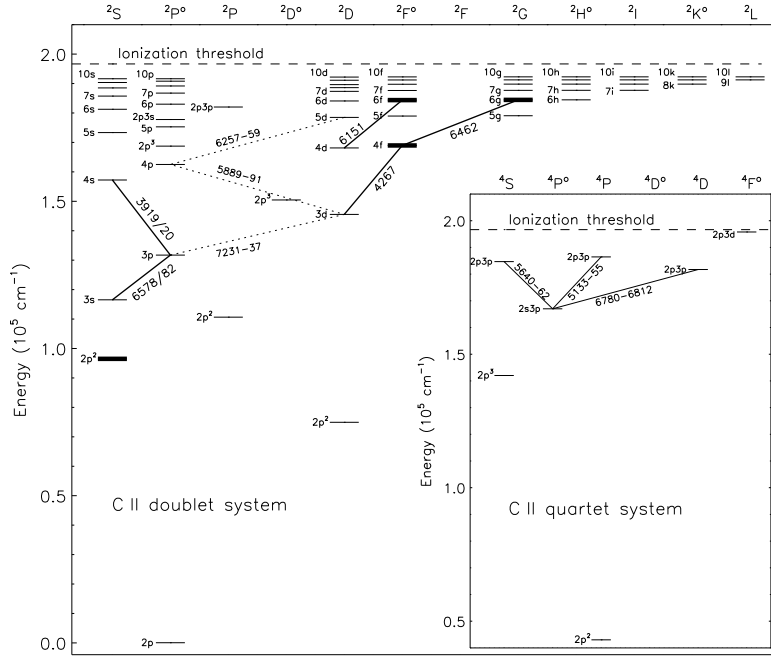


Fig. 8. Grotrian diagram for the C II doublet and quartet spin systems. Transitions that give rise to lines in the optical spectra of B-type stars are identified by continuous and dotted lines. These are the observables available for testing model atoms. Additional channels become available in the UV and IR spectral range. From NP08.

This is in order to test the reaction of the model realisations to a hardening radiation field. The line ‘in LTE’ serves as reference and the goal of the model atom optimisation is to minimise the differences in the derived abundances from the various indicators. In this case it was shown that ill-chosen atomic data can result in line abundance differing by up to 0.8 dex (NP08), which helped to solve one notorious non-LTE problem of stellar astrophysics (Nieva & Przybilla 2006).

Ideally, the observations used for the model atom calibration should range from the far-UV to the near-IR in order to test as many channels (spectral lines) as possible, even those that may be irrelevant for practical applications later. At the same time, the observations should cover an as wide range of plasma parameters as possible: high-density, i.e. collisionally dominated, environments like the photospheres of dwarf stars and low-density plasmas (those dominated by radiative processes) as encountered in (super-)giants should be considered, at different temperatures. Where possible, also the metallicity dependence of non-LTE effects should be investigated to test the response of a model atom to a varying radiation field, e.g. by considering stars of Population I and II. Further tests may include more ‘exotic’ environments, like He-dominated plasmas in compact subdwarfs (Przybilla et al. 2006a) or giant extreme helium stars (Przybilla et al. 2005, 2006b).

Such a comprehensive approach involving satellite observations may not be feasible in almost all cases. However, high-quality spectroscopy from the ground with modern echelle spectrographs is often sufficient to provide the means to facilitate proper model atom testing. Figure 8 visualises the channels available for testing a model atom of C II using the optical spectra of early B-type stars. Note that despite this comprises a fair number of energy levels and transitions from several multiplets, only a small fraction of the entire model atom can be really scrutinised by this. Consideration of lines from additional ionization stages (C III and C IV in that case, NP08) may put further constraints, as the full set of observed lines should be reproduced closely by the model simultaneously.

The above example is typical for elements with relatively simple electron structure. More complex electron configurations like the open $3d$ -shells in the iron-group members pose a larger challenge at first glance, but the enormous number of observable transitions puts many constraints on the model atom construction as well. The real challenge are therefore the low-abundance light elements lithium, beryllium and boron, and in particular their alkali-like ions⁵. There, typically only the resonance lines are observable, which gives only marginal constraints for tests of the model atom. Where possible, resonance lines from another ionization stage should therefore be investigated, or subordinate lines that may become observable in stars with particular high abundance in the element under study.

It is of utmost importance to use realistic atmospheric structures for testing model atoms, requiring a proper determination of the stellar atmospheric parameters, see Nieva & Przybilla (this volume). Well-studied standard stars like the Sun (G2 V), Procyon (F5 IV-V), Vega (A0 V), τ Sco (B0.2 V) or Arcturus (K1.5 III) with tight constraints on their atmospheric parameters are therefore primary objects for the comparison of the models with observation. However, further stars that bracket the extremes of the parameter space to be studied have also to be considered.

8 Final Remarks

The plethora of possibilities implies that the model atom construction does not result in a unique solution. A good reproduction of observations may be achieved by a whole family of models. The main insight is that there are many insufficient model atoms, but few adequate ones. In consequence, non-LTE analyses are not superior to LTE investigations *per se*, but require robust and comprehensive model atoms. In view of the increasing availability of accurate and precise atomic data from *ab-initio* calculations and experiments one is faced by a perpetual challenge: the impact of new high-quality atomic data should be tested on the modelling whenever such become available. Of course, the same is true for new observations that may facilitate the predictive power of the models to be tested further by opening up other channels for the model atom calibration.

⁵High-quality atomic data can fortunately be obtained with relative ease for these simple ions.

References

- Allen, C. 1973, *"Astrophysical Quantities"*, 3rd edn. (Athlone Press: London)
- Anderson, L. S. 1989, ApJ, 339, 558
- Arnaud, M. & Rothenflug, R. 1985, A&AS, 60, 425
- Auer, L. & Mihalas, D. 1973, ApJ, 184, 151
- Badnell, N. R., O'Mullane, M. G., Summers, H. P., et al. 2003, A&A, 406, 1151
- Barklem, P. S. 2007, A&A, 466, 327
- Baschek, B., Scholz, M. & Sedlmayr, E. 1977, A&A, 55, 375
- Belyaev, A. K., Grosser, J., Hahne, J. & Menzel, T. 1999, Phys. Rev. A, 60, 2151
- Belyaev, A. K. & Barklem, P. S. 2003, Phys. Rev. A, 68, 062703
- Belyaev, A. K., Barklem, P. S., Dickinson, A. S. & Gadéa, F. X. 2010, Phys. Rev. A, 81, 032706
- Bray, I., Fursa, D. V., Kheifets, A. S. & Stelbovics, A. T. 2002, J. Phys. B, 35, R117
- De Marco, O., Storey, P. J. & Barlow, M. J. 1998, MNRAS, 297, 999
- Drawin, H. W. 1961, Z. Physik, 164, 513
- Drawin, H. W. 1968, Z. Physik, 211, 404
- Drawin, H. W. 1969, Z. Physik, 225, 483
- Fabbian, D., Asplund, M., Barklem, P. S., et al. 2009, A&A, 500, 1221
- Fleck, I., Grosser, J., Schneck, A., et al. 1991, J. Phys. B, 24, 4017
- Froese Fischer, C. & Tachiev, G. 2004, At. Data Nucl. Data Tables, 87, 1
- Hummer D. G., Berrington K. A., Eissner W., et al. 1993, A&A, 279, 298
- Kjeldsen, H. 2006, J. Phys. B, 39, R325
- Kurucz, R. L. 2006, EAS Pub. Ser., 18, 129
- Mashonkina, L. J. 1996, in *"Model Atmospheres and Spectrum Synthesis"*, ed. S. J. Adelman, F. Kupka & W. W. Weiss (ASP: San Francisco), p. 140
- Mihalas, D. 1972, ApJ, 177, 115
- Mihalas, D. 1978, *"Stellar Atmospheres"*, 2nd ed. (W.H. Freeman & Co: San Francisco)
- Nahar, S. & Pradhan, A. 1997, ApJS, 111, 339
- Nahar, S. 2002, At. Data Nucl. Data Tables, 80, 205
- Nieva, M. F. & Przybilla, N. 2006, ApJ, 639, L39
- Nieva, M. F. & Przybilla, N. 2008, A&A, 481, 199 (NP08)
- Przybilla, N. & Butler, K. 2004, ApJ, 609, 1181
- Przybilla, N., Butler, K., Becker, S. R., et al. 2000, A&A, 359, 1085
- Przybilla, N., Butler, K., Becker, S. R. & Kudritzki, R. P. 2001, A&A, 369, 1009
- Przybilla, N., Butler, K., Heber, U. & Jeffery, C. S. 2005, A&A, 443, L25
- Przybilla, N., Nieva, M. F. & Edelmann, H. 2006a, Balt. Astron., 15, 107
- Przybilla, N., Nieva, M. F., Heber, U. & Jeffery, C. S. 2006b, Balt. Astron., 15, 163
- Seaton, M. J. 1962, in *"Atomic and Molecular Processes"* (Academic Press: New York)
- Seaton, M. J. 1987, J. Phys. B, 20, 6363
- Seaton, M. J., Yu, Y., Mihalas, D. & Pradhan A. K. 1994, MNRAS, 266, 805
- Sigut, T. A. A. 1996, ApJ, 473, 452
- Steenbock, W. & Holweger, H. 1984, A&A, 130, 319

- Takeda, Y. 1991, *A&A*, 242, 455
Van Regemorter, H. 1962, *ApJ*, 136, 906
Williams, I. D. 1999, *Rep. Prog. Phys.*, 62, 1431
Wilson, N. J., Bell, K. L. & Hudson, C. E. 2005, *A&A*, 432, 731
Yan, Y. & Seaton, M. J. 1987, *J. Phys. B*, 20, 6409
Yan, Y., Taylor, K. T. & Seaton, M. J. 1987, *J. Phys. B*, 20, 6399